Computation insight of modified thermal distribution of hybrid nanofluids in complex wavy channel: A comparative thermal approach for different nanofluid models

Imtiaz Ahmed[a], Shahid Hameed[a], Aamar Abbasi[b], Sami Ullah Khan[c,*], Waseh Farooq[b], Mohammed A. Almeshaal[d], Muapper Alhadri[e], Lioua Kolsi[e,f]

[a]Department of Mathematics, Mirpur university of Science and Technology, Mirpur Pakistan

[b]Department of Mathematics, University of Azad Jammu and Kashmir Muzaffarabad, Pakistan

[c,*]Department of Mathematics, Namal University, Mianwali 42250, Pakistan

[d] Department of Mechanical Engineering, College of Engineering, Imam Mohammad Ibn Saud Islamic University, Riyadh 11432, Saudi Arabia

[e] Department of Mechanical Engineering, College of Engineering, University of Ha'il, Ha'il City 81451, Saudi Arabia

[f] Laboratory of Meteorology and Energy Systems, University of Monastir, Monastir 5000, Tunisia

***Corresponding author:** sk_iiu@yahoo.com (+923137141665)

Abstract: Owing to enhanced thermal mechanism of nanomaterials, the researchers are continuously exploring the novel features of nanofluids and claiming multidisciplinary applications in solar systems, engineering processes, energy devices and automobile industries. The experimentally supported research proves that with interaction of different types of nanoparticles is more effective to enhance the thermal transportation phenomenon. Following such motivations in mind, the aim of present continuation is exploring the thermal impact of modified hybrid nanofluid model in complex vertical channel. Due to high thermal performances, copper (CuO), copper oxide (CuO) and aluminum oxide (Al_2O_3) nanoparticles explore the thermal behavior of modified hybrid nanofluid model. The vertical channel confined the sinusoidal waves on walls. The flow phenomenon is based on peristaltic transport associated to the human body system. The consideration of small Reynolds number hypothesis and larger wavelength approach, the implication of problem has been done. The modeled equations are tackled with shooting technique. Various stream functions with applications of peristaltic transport phenomenon are developed. It is observed that heat transfer is larger in the curved channel as compared to the straight channel. The

decomposition of modified hybrid nanoparticles is more effective to improve the heat transfer pattern more effectively.

Keywords: Modified hybrid nanofluid; peristaltic phenomenon; complex wavy channel; mixed convection; numerical technique.

1. Introduction

The improved thermal aspect of nanomaterials convinced the scientists to continue research on this topic and suggest different applications in multidisciplinary way. The attention of nanoparticles is important as such materials enhanced the thermal properties of base fluids. The heating phenomenon is the most basic and fundamental aspect in industrial and engineering processes. For achieving different quality products, the control of heat transfer is important. The continuing research in nanotechnology attributed the role of nanofluids for enhancing the heat transportation phenomenon exclusively. The nanomaterials are basically metallic materials of small shape with justified properties. Different applications of nanofluids is claimed in modern technology, solar systems, cooling of different objects, engine oil, diesel generators etc. Choi [1] reported the experimental supported based achievements for nanofluids and provides the direction towards this topic. Boungiorno [2] claimed the Brownian aspect of nanofluids along with thermophoretic effects. Turkyilmazoglu [3] stated the hydrodynamical onset of nanoparticles with ensured thermal impact. Khan et al. [4] discussed the heating improvement aspect of third grade nanofluid which was indorsed due to oscillating uniform surface. Ibrahim and Gizewu [5] attributed the role of mixed convection for nanofluid flow along with tangent hyperbolic fluid. Tayebi et al. [6] identified the CNTs thermal association with water base liquid referring to the uniform heat flux. Hayat et al. [7] reported the novel thermal contribution of Williamson nanofluid with justified optimized framework. Eyring-Powell thermal exploration of nanofluid justifying the chemical reactive species was discussed by Khan et al. [8]. The computational framework for bioconvective approach of nanofluid has been reported in the flow model of Khan et al. [9]. Mondal and Pal [10] tested the variable viscosity effects for enhancing the nanofluid properties. Gowda et al. [11] reported a spinning pattern of nanofluids with thermal decomposition. Acharya [12] disclosed the heat transmission of nanofluid referred by cavity with stable hydrothermal prospective. Patil et al. [13] depicted the triple diffusion aspect of nanofluid due to wedge surface. The thermal influence of heat fluctuation characteristics under the roughness of sphere was reported by Patil et al. [14].

The hybrid nanofluid is a new extended sub-category of nanofluids which export more stable thermal behavior. The reorganization of hybrid nanofluids deals with two different nanoparticles decomposition with base material. More strengthen thermal outcomes of hybrid nanofluid model are achieved as two distinct nanoparticles collectively enhanced the base material properties. Moreover, stronger chemical bonding is resulted for interaction of hybrid nanoparticles. The enhanced features of hybrid nanofluids reports applications in the energy management systems, vehicle cooling phenomenon, manufacturing systems, solar production etc. Acharya [15] tested the role of hybrid nanofluid due to heated enclosure having fins and inspected the improve thermal impact. Madhukesh et al. [16] recognized thermal influence of hybrid nanoparticles with Newtonian heating phenomenon. Sannad et al. [17] observed the cavity flow loaded with hybrid nanoparticles attaining the natural convective flow. The computational insight heating prosperities of hybrid nanofluid with FEM approach. Ali et al. [18] decomposed the viscous dissipation supported hybrid nanomaterial flow containing the copper and aluminium nanoparticles. The experimental approach of hybrid nanofluid flow with distribution of shear thinning material was intended by Hassan et al. [19]. Bhatti and Abdelsalam [20] explored the inspired thermal source of hybrid nanoparticles with bio-medical applications. Hamrelaine et al. [21] reported the divergent channel flow with ferro nanoparticles and computed analytical results. Shahzad et al. [22] disclosed the tri-hybrid nanofluid thermal effectives in circular channel under the deviation of pressure gradient effects. Sajid et al. [23] observed the decomposed aspect of hybrid nanofluid with Reiner-Philippoff model. Hanif et al. [24] used the Crank-Nicolson scheme to report the aluminium hybrid nanoparticles in horizontal plate. The investigation claiming the trihybrid Casson nanofluid thermal aspect owing to the Bödewadt flow was utilized by Sajid et al. [25]. Patil and Goudar [26] observed the hybrid nanofluid aspect for rough surface flow due to cone. Patil et al. [27] focused on the natural convection of silica–molybdenum disulphide decomposition with hybrid nanoparticles. Patil and Shankar [28] presented the aluminium oxide and ion nanoparticles thermal assessment with water decomposed based liquid over yawed cylinder. Patil and Benawadi [29] explained the shape features for convective thermal hybrid nanofluid flow subject to the slender cylinder.

The modified hybrid nanofluid is the collection of more than two distinct nanoparticles with suspension of base fluids. In fact, to enhance the high thermal achievements, the scientists successfully utilized the decomposition of more than two nanoparticles to get enhance transfer rate. This improved class is known as modified hybrid nanofluids. Some contributions on modified hybrid nanofluid is presented in research [30-32].

The peristaltic is a process in which physiological fluid is pushed by means of sinusoidal waves proceeding axially along the extent of tube. Peristaltic flows at low Reynolds number and long wavelength have reached expand to allow ended the years. There are many applications such as medical sciences and engineering. Such as transport of food, some blood vessel, movement of spermatozoa, urine from kidney to the bladder, moves food through digestive tract. Some applications referring to the peristaltic transport are observed in the biomedical sciences, drugs, heart pumping and heart lung machine. Owing to importance of peristaltic phenomenon, several investigations are provided in literature. Ramesh et al. [33] depicted the peristaltic mechanism carrying out for viscoelastic fluid with electro-osmotic significance. Rafaqat et al. [34] considered the second-grade fluid for wavy type channel flow with associated to the energy storage systems. Ullah et al. [35] contributed the role of ion slip and joule heating effects while contributing the phenomenon of peristaltic transport for PTT model. The applications of peristaltic transfer with interaction of nanoparticles is also intended by researchers. For instance, Bibi and Xu [36] discussed the optimization of nanofluid regarding the peristalsis flow in horizontal channel. Ali et al. [37] discussed the diffusion aspect of nanofluid in channel having deformable walls. Tripathi et al. [38] reported the role of nanofluid following the peristaltic behavior in drug delivery systems. The curved channel supported with peristaltic transport was inspected by Tanveer et al. [39]. Bibi and Xu [40] directed a computation investigation for the hybrid nanofluid analysis for peristalsis flow referring to reactive e materials. Tanveer et al. [41] examined the Sisko nanofluid in curved geometry with addition of hybrid nanoparticles. Alhazmi et al. [42] explored the fundamental of peristalsis phenomenon with nanofluid. McCash et al. [43] contributed the mathematical modelling for hybrid nanofluid in elliptic channel with peristalsis behavior. The hybrid nanofluid for peristaltic flow in rectangular channel with explanation of eigenfunction was defined by Nadeem et al. [44]. McCash et al. [45] performed entropy generation on set for peristaltically moving hybrid nanoparticles flow in elliptic duct.

After successfully presenting a detail literature on the nanofluids flow with phenomenon, it is noticed that different investigations are performed on this topic with diverse flow features. In maximum investigations, the researchers have focused on inspecting the heat transfer phenomenon by using the hybrid nanofluid associated to the peristaltic transport phenomenon. However, no computational model is presented for investigating the enhancing the thermal attention for peristaltic transport due to interaction of modified hybrid nanoparticles in curved channel. Therefore, the objective of current investigation is to present a computational thermal impact of modified hybrid nanofluid for a peristaltic transport in

curved channel. The thermal impact of modified hybrid nanofluid consisting of copper (CuO), copper oxide (CuO) and aluminium oxide (Al_2O_3) nanoparticles. The mixed convection prospective of nanofluid flow is also attributed. The mathematical expressions and different nanoparticles are justified. The curved channel motion is based on the movement of sinusoidal waves of walls. A comparative computational outcome for nanofluid, hybrid nanofluid and modified hybrid nanofluid model is performed.

2. Problem formulation

The motion of modified hybrid nanofluid in a non-uniform curved channel of width 2b as shown in Fig. 1 is taken into account. The motion is produced by the mean pressure gradient and the propagation of the waves on the walls of the channel. The orthogonal curvilinear coordinates $(\bar{R},\ \bar{X})$ are chosen in such a way that $\bar{R}$ is radial and $\bar{X}$ is axial direction. The magnetic field of strength B_0 acting in radial direction. The electric field is negligible and magnetic Reynolds number is assumed to be very small. The left wall $\bar{H}_1$ and right wall $\bar{H}_2$ of the channel are maintained at uniform temperature $\bar{T}_1$ and $\bar{T}_0$ respectively. The mathematical representation of the walls is:

$$\bar{H}_1\left(\bar{X},\bar{t}\right)=-b-\bar{M}\left(\bar{X}-c\bar{t}\right)-\begin{bmatrix}\bar{a}_1\sin\left(\frac{2\sigma\pi}{\lambda}\left(\bar{X}-c\bar{t}\right)+\sigma\zeta\right)\\-\bar{a}_2\sin\left(\frac{2\omega\pi}{\lambda}\left(\bar{X}-c\bar{t}\right)+\omega\zeta\right)\end{bmatrix}, \tag{1}$$

$$\bar{H}_2\left(\bar{X},\bar{t}\right)=b+\bar{M}\left(\bar{X}-c\bar{t}\right)+\bar{a}_1\sin\left(\frac{2\sigma\pi}{\lambda}\left(\bar{X}-c\bar{t}\right)\right)+\bar{a}_2\sin\left(\frac{2\omega\pi}{\lambda}\left(\bar{X}-c\bar{t}\right)\right). \tag{2}$$

In above c is the speed of sinusoidal wave, λ is the wave length, ζ is phase difference, $(\bar{a}_{i,}\, i=1,2)$ are wave amplitudes, σ and ω are geometrical parameters and $\bar{t}$ denotes the time.

For an incompressible fluid the mass, momentum and energy conservation laws give rise the equations.

Continuity equation:

$$\frac{\partial}{\partial\bar{R}}\left\{\left(\bar{R}+R^*\right)\bar{V}\right\}+R^*\frac{\partial\bar{U}}{\partial\bar{X}}=0, \tag{3}$$

The radial component of the momentum equation:

$$\rho_m\left[\begin{array}{l}\dfrac{\partial \overline{V}}{\partial \overline{t}}+\dfrac{R^*\overline{U}}{R^*+\overline{R}}\dfrac{\partial \overline{V}}{\partial \overline{X}}\\ +\overline{V}\dfrac{\partial \overline{V}}{\partial \overline{R}}-\dfrac{\overline{U}^2}{R^*+\overline{R}}\end{array}\right]=-\frac{\partial \overline{P}}{\partial \overline{R}}+\mu_m\left(\begin{array}{l}\left(\dfrac{1}{R^*+\overline{R}}\right)\dfrac{\partial}{\partial \overline{R}}\left(\left(R^*+\overline{R}\right)\dfrac{\partial \overline{V}}{\partial \overline{R}}\right)-\dfrac{\overline{V}}{\left(R^*+\overline{R}\right)^2}\\ +\left(\dfrac{R^*}{R^*+\overline{R}}\right)^2\dfrac{\partial^2\overline{V}}{\partial \overline{X}^2}-\dfrac{2R^*}{\left(R^*+\overline{R}\right)^2}\dfrac{\partial \overline{U}}{\partial \overline{X}}\end{array}\right), \tag{4}$$

Axial component of momentum equation:

$$\rho_m\left[\begin{array}{l}\dfrac{\partial \overline{U}}{\partial \overline{t}}+\dfrac{R^*\overline{U}}{R^*+\overline{R}}\dfrac{\partial \overline{U}}{\partial \overline{X}}\\ +\overline{V}\dfrac{\partial \overline{U}}{\partial \overline{R}}-\dfrac{\overline{U}^2\overline{V}}{R^*+\overline{R}}\end{array}\right]=-\frac{\overline{R}}{R^*+\overline{R}}\frac{\partial \overline{P}}{\partial \overline{X}}+\mu_m\left[\begin{array}{l}\dfrac{1}{R^*+\overline{R}}\dfrac{\partial}{\partial \overline{R}}\left\{\left(R^*+\overline{R}\right)\dfrac{\partial \overline{U}}{\partial \overline{R}}\right\}-\dfrac{\overline{U}}{\left(R^*+\overline{R}\right)^2}\\ +\left(\dfrac{R^*}{R^*+\overline{R}}\right)^2\dfrac{\partial^2\overline{U}}{\partial \overline{X}^2}-\dfrac{2R^*}{\left(R^*+\overline{R}\right)^2}\dfrac{\partial \overline{V}}{\partial \overline{X}}\end{array}\right] \tag{5}$$

$$-\frac{\sigma_m B_0^2 R^{*2}\overline{U}}{\left(\overline{R}+R^*\right)^2}+g\left(\rho\beta\right)_m\left(\overline{T}-T_0\right),$$

Energy equation with viscous dissipation is:

$$\begin{aligned}&\left(\rho c\rho\right)_m\left(\frac{\partial \overline{T}}{\partial \overline{t}}+\overline{V}\frac{\partial \overline{T}}{\partial \overline{R}}+\frac{R^*\overline{U}}{R^*+\overline{R}}\frac{\partial \overline{T}}{\partial \overline{X}}\right)=K_m\left[\frac{1}{R^*+\overline{R}}\frac{\partial}{\partial \overline{R}}\left\{\left(R^*+\overline{R}\right)\frac{\partial \overline{T}}{\partial \overline{R}}\right\}+\left(\frac{R^*}{R^*+\overline{R}}\right)^2\frac{\partial^2\overline{T}}{\partial \overline{X}^2}\right]\\ &+\mu_m\left[\left(2\left(\frac{\partial \overline{V}}{\partial \overline{R}}\right)^2+\frac{R^*}{\left(R^*+\overline{R}\right)^2}\frac{\partial \overline{U}}{\partial \overline{X}}+\frac{\overline{V}}{R^*+\overline{R}}\right)+\left(\frac{\partial \overline{U}}{\partial \overline{R}}+\frac{R^*}{R^*+\overline{R}}\frac{\partial \overline{V}}{\partial \overline{X}}-\frac{\overline{U}}{R^*+\overline{R}}\right)\right]^2\end{aligned} \tag{6}$$

In above $\overline{V}$ and $\overline{U}$ are the components of velocity $\overline{P}$ is a pressure, R^* is radius of curvature, μ_m is viscosity , $\left(\rho cp\right)_m$ is heat capacity, ρ_m is density, K_m is thermal conductivity $\overline{T}$, is a temperature, σ_m is electric conductivity and $\left(\beta\right)_m$ is thermal expansion coefficient of modified hybrid nanofluid. These quantities satisfy the following relations [21, 22].

$$\mu_m=\mu_f\left(1-\left(\sum_{i=1}^{3}\phi_i\right)\right)^{-2.5}, \tag{7}$$

$$\rho_m=\left(1-\left(\sum_{i=1}^{3}\phi_i\right)\right)\rho_f+\sum_{i=1}^{3}\phi_i\rho_{S_i}, \tag{8}$$

$$\left(\rho c\rho\right)_m=\left(1-\left(\sum_{i=1}^{3}\phi_i\right)\right)\left(\rho C_p\right)_f+\sum_{i=1}^{3}\phi_i\left(\rho C_p\right)_{S_i}, \tag{9}$$

$$(\rho\beta)_m = \left(1-\left(\sum_{i=1}^{3}\phi_i\right)\right)(\rho\beta)_f + \sum_{i=1}^{3}\phi_i(\rho\beta)_{S_i}, \tag{10}$$

$$K_m = \frac{\left(\sum_{i=1}^{3}(\phi_i K_i)\right)+2\sum_{i=1}^{3}\phi_i K_f + 2\left(\sum_{i=1}^{3}\phi_i\right)\left(\sum_{i=1}^{3}\phi_i K_i\right)-2\left(\sum_{i=1}^{3}\phi_i\right)^2 K_f}{\left(\sum_{i=1}^{3}(\phi_i K_i)\right)+2\sum_{i=1}^{3}\phi_i K_f - \left(\sum_{i=1}^{3}\phi_i\right)\left(\sum_{i=1}^{3}\phi_i K_i\right)+\left(\sum_{i=1}^{3}\phi_i\right)^2 K_f} K_f, \tag{11}$$

$$\sigma_m = \frac{\left(\sigma_{S_3}+2\sigma_{hnf}-2\phi_3\left(\sigma_{hnf}-\sigma_{S_3}\right)\right)\left(\sigma_{S_2}+2\sigma_{nf}-2\phi_2\left(\sigma_{nf}-\sigma_{S_2}\right)\right)\left(\sigma_{S_1}+2\sigma_f-2\phi_1\left(\sigma_f-\sigma_{S_1}\right)\right)}{\left(\sigma_{S_3}+2\sigma_{hnf}+\phi_3\left(\sigma_{hnf}-\sigma_{S_3}\right)\right)\left(\sigma_{S_2}+2\sigma_{nf}+\phi_2\left(\sigma_{nf}-\sigma_{S_2}\right)\right)\left(\sigma_{S_1}+2\sigma_f+2\phi_1\left(\sigma_f-\sigma_{S_1}\right)\right)}\sigma_f. \tag{12}$$

In above relations (ϕ_1, ϕ_2, ϕ_2) are solid volume fractions of (CuO, Cu, Al_2O_3), $(\sigma_f, \sigma_{s_1}, \sigma_{s_2}, \sigma_{s_3})$ are electric conductivities $(\rho_f, \rho_{s_1}, \rho_{s_2}, \rho_{s_3})$ are densities, $\left((C_p)_f, (C_p)_{s_1}, (C_p)_{s_2}, (C_p)_{s_3}\right)$ are heat capacities, $(\beta_f, \beta_{s_1}, \beta_{s_2}, \beta_{s_3})$ are thermal expansion coefficients, (K_f, K_1, K_2, K_2) are thermal conductivities of (H_2O, CuO, Cu, Al_2O_3) the experimentally verified values of theses quantities are expresses in the **Table 1**.

2.1 Boundary conditions

The suitable no-slip boundary conditions satisfied by the velocity components and the temperature are

$$\overline{U}=0, \overline{V}=\frac{\partial\overline{H_1}}{\partial t}, T=T_1 \text{ at } R=\overline{H_1} \text{ and } \overline{U}=0, \overline{V}=\frac{\partial\overline{H_2}}{\partial t}, T=T_0 \text{ at } R=\overline{H_2}. \tag{13}$$

It is evident that flow is unsteady in $(\bar{R}, \bar{X})$ (laboratory frame) and is considered as steady a coordinates system $(\bar{x}, \bar{r})$ (Wave frame)**.** The set of linear transformations relates both the coordinate system are

$$\bar{r}=\overline{R}, \bar{x}=\overline{X}-c\bar{t}, \bar{u}=\overline{U}-c, \bar{v}=\overline{V}, \overline{T}=T, \tag{14}$$

The governing eqns. (3-6) with velocity components $\bar{u}, \bar{v}$ in wave frame can be written as

$$\frac{\partial}{\partial\bar{r}}\left\{\left(\bar{r}+R^*\right)\bar{v}\right\}+R^*\frac{\partial\bar{u}}{\partial\bar{x}}=0, \tag{15}$$

$$\rho_m\begin{bmatrix} -c\dfrac{\partial \bar{v}}{\partial \bar{x}}+\dfrac{R^*\left(\bar{u}+c\right)}{R^*+\bar{r}}\dfrac{\partial \bar{v}}{\partial \bar{x}} \\ +\bar{v}\dfrac{\partial \bar{v}}{\partial \bar{r}}-\dfrac{\left(\bar{u}+c\right)^2}{R^*+\bar{r}} \end{bmatrix}=-\frac{\partial \bar{p}}{\partial \bar{r}}+\mu_m\begin{pmatrix} \dfrac{1}{R^*+\bar{r}}\dfrac{\partial}{\partial \bar{r}}\left(\left(R^*+\bar{r}\right)\dfrac{\partial \bar{v}}{\partial \bar{r}}\right)+\left(\dfrac{R^*}{R^*+\bar{R}}\right)^2\dfrac{\partial^2 \bar{v}}{\partial \bar{x}^2} \\ -\dfrac{\bar{v}}{\left(R^*+\bar{r}\right)^2}-\dfrac{2R^*}{\left(R^*+\bar{R}\right)^2}\dfrac{\partial \bar{u}}{\partial \bar{x}} \end{pmatrix}, \tag{16}$$

$$\rho_m\begin{bmatrix} -c\dfrac{\partial \bar{u}}{\partial \bar{x}}+\dfrac{R^*\left(\bar{u}+c\right)}{R^*+\bar{r}}\dfrac{\partial \bar{u}}{\partial \bar{x}} \\ +\bar{v}\dfrac{\partial \bar{u}}{\partial \bar{r}}-\dfrac{\left(\bar{u}+c\right)\bar{v}}{R^*+\bar{r}} \end{bmatrix}=-\frac{\bar{R}}{R^*+\bar{r}}\frac{\partial \bar{p}}{\partial \bar{x}}+\mu_{mf}\begin{pmatrix} \dfrac{1}{R^*+\bar{r}}\dfrac{\partial}{\partial \bar{r}}\left(\left(R^*+\bar{r}\right)\dfrac{\partial \bar{u}}{\partial \bar{r}}\right)+\left(\dfrac{R^*}{R^*+\bar{r}}\right)^2\dfrac{\partial^2 \bar{u}}{\partial \bar{x}^2} \\ -\dfrac{\left(\bar{u}+c\right)}{\left(R^*+\bar{R}\right)^2}-\dfrac{2R^*}{\left(R^*+\bar{r}\right)^2} \end{pmatrix} \tag{17}$$

$$-\frac{\sigma_m B_0^2 R^{*2}\left(\bar{u}+c\right)}{\left(\bar{r}+R^*\right)^2}+g\left(\rho\beta\right)_m\left(T-T_0\right),$$

$$\left(\rho c\rho\right)_m\left(-c\frac{\partial T}{\partial \bar{x}}+\bar{v}\frac{\partial T}{\partial \bar{r}}+\frac{R^*\left(\bar{u}+c\right)}{R^*+\bar{r}}\frac{\partial T}{\partial \bar{x}}\right)=K_m\left[\frac{1}{R^*+\bar{r}}\frac{\partial}{\partial \bar{r}}\left\{\left(R^*+\bar{r}\right)\frac{\partial T}{\partial \bar{r}}\right\}+\left(\frac{R^*}{R^*+\bar{r}}\right)^2\frac{\partial^2 T}{\partial \bar{x}^2}\right] \tag{18}$$

$$+\mu_m\left[\left(2\left(\frac{\partial \bar{v}}{\partial \bar{r}}\right)^2+\frac{R^*}{\left(R^*+\bar{r}\right)^2}\frac{\partial \bar{u}}{\partial \bar{x}}+\frac{\bar{v}}{R^*+\bar{r}}\right)+\left(\frac{\partial \bar{u}}{\partial \bar{r}}+\frac{R^*}{R^*+\bar{r}}\frac{\partial \bar{v}}{\partial \bar{x}}-\frac{\left(\bar{u}+c\right)}{R^*+\bar{r}}\right)\right]^2$$

2.2 Dimension less formulation

In order to normalized the above equations, we introduced the following scale variables

$$x=\frac{2\pi \bar{x}}{\lambda},\quad \eta=\bar{r}/b,\quad u=\bar{u}/c,\quad v=\bar{v}/c,\quad \overline{P}=\left(2\pi b^2\right)/\left(\lambda\mu_f c\right)\bar{p},\quad h_1=\overline{H}_1/b,\quad h_2=\overline{H}_2/b,$$

$$a_1=\bar{a}_1/b,\ b_1=\bar{a}_2/b, \tag{19}$$

Invoking the scaled variables introduced in (19) after ignoring the bars $(-)$ and introducing the stream function $u=-\partial\psi/\partial\eta,\ v=\delta\dfrac{k}{\eta+k}\dfrac{\partial\psi}{\partial x}$ the continuity equation (15) is satisfy and applying the wildly used assumptions of long wave length and low Reynolds number, the equations (16-19) takes the form

$$\partial p/\partial\eta=0, \tag{20}$$

$$-\frac{\partial p}{\partial x}=\frac{\mu_m}{\mu_f}\left(\frac{\partial}{\partial\eta}\left(\eta+k\right)\frac{\partial^2\psi}{\partial\eta^2}-\frac{1}{\eta+k}\left(1-\frac{\partial\psi}{\partial\eta}\right)\right)+\frac{\left(\rho\beta\right)_m}{\left(\rho\beta\right)_f}Gr_t\theta+Ha^2\frac{\sigma_m}{\sigma_f}\frac{k^2}{\left(\eta+k\right)^2}\left(1-\frac{\partial\psi}{\partial\eta}\right), \tag{21}$$

$$\frac{K_m}{k_f}\left(\theta^{"}+\frac{1}{\eta+k}\theta'\right)+\frac{Br\mu_m}{\mu_f}\left(\frac{\partial^2\psi}{\partial\eta^2}+\frac{1}{\eta+k}\left(1-\frac{\partial\psi}{\partial\eta}\right)\right)^2=0.. \tag{22}$$

With the Boundary conditions in a wave frame are

$$\frac{\partial\psi}{\partial\eta}=1,\theta=1 \text{ at } \eta=h_2=1+m\bar{x}+a_1 sin\sigma x+b_1 sin\omega x \tag{23}$$

$$\frac{\partial\psi}{\partial\eta}=1,\ \theta=0 \text{ at } \eta=h_1=-1-m\bar{x}-a_1 sin\sigma\left(x+\phi\right)-b_1 sin\omega\left(x+\phi\right) \tag{24}$$

In above equations $m=\bar{M}/b$ is non-uniform parameter $E_C=c^2/c_f\left(T_1-T_0\right)$ is Eckert number $p_r=\mu_f c_{f/K_f}$ is Prandtl number and $B_r=E_c p_r$. $Gr_t=g\left(\rho\beta\right)_f\left(T_1-T_0\right)b^2/c\mu_f$ is thermal Grashof number and $Ha^2=B_0^2b^2\sigma_f/\mu_f$ is magnetic parameter frequently known as Hartman number. Eliminating the pressure from equations (20-21) a fourth order ordinary equation of the form is obtained.

$$\frac{\mu_m}{\mu_f}\frac{\partial}{\partial\eta}\left(\left(\frac{\partial}{\partial\eta}\left(\eta+k\right)\frac{\partial^2\psi}{\partial\eta^2}-\frac{1}{\eta+k}\left(1-\frac{\partial\psi}{\partial\eta}\right)\right)+\frac{\left(\rho\beta\right)_m}{\left(\rho\beta\right)_f}Gr_t\theta+Ha^2\frac{\sigma_m}{\sigma_f}\frac{k^2}{\left(\eta+k\right)^2}\left(1-\frac{\partial\psi}{\partial\eta}\right)\right)=0, \tag{25}$$

The boundary conditions (23-24) are not sufficient for the solution of equation (25) so in order to obtain the missing conditions we defined the addition condition that at each cross-section the flow rate is constant. In view of this assumption the missing boundary conditions can be obtained in the following form

$$\psi=-\frac{q}{2} \ at \ \eta=h_2 \ \text{ and } \psi=\frac{q}{2} \ at \ \eta=h_1. \tag{26}$$

Where q is dimensionless mean flow in wave frame.

3. Solution methodology

It is very difficult to solve analytically the dimensionless governing equations (21and 25) subject to boundary conditions (23,24,26). Many techniques are proposed and used by scientists to compute such types of equations by various numerical methods. In present study, shooting method is used to solve the coupled system of differential equations. The motivations for implementing shooting scheme are due to higher accuracy. This method does

not involve complicated discretization like other numerical computations. The accuracy of results is ensured with 10^{-4}.

4. Results and Discussion

This section deals with the graphical description of various peristaltic flow features like axial velocity, streamlines, axial pressure and temperature for three types of fluid under consideration CuO nanofluid $(\phi\_1 = 0.04, \phi\_2 = 0 = \phi\_3)$, $CuO + Cu$ hybrid nanofluid $(\phi_1 = 0.04, \phi_2 = 0.05, \phi_3 = 0.0)$ and modified hybrid nanofluid $(\phi_1 = 0.04, \phi_2 = 0.05 = \phi_3)$.

4.1 Flow analysis

Fig. 2 is plotted to analyze the response of axial velocity against the Hartman number Ha for three types of different nanofluids under consideration. It is noted that the axial velocity $u(\eta)$ reduces in the left half of the channel for all types of nanofluids under consideration. Furthermore, the rise in axial velocity is noted against Hartman number and phenomena of Hartman boundary layer is observed in the right half of the channel. The similar response of axial velocity is noted against the thermal Grashof number Gr_t for various nanofluids under consideration (Fig. 3). Also, the velocity is maximum magnitude in the left half for CuO nanoparticles as compared to hybrid nanofluid and modified hybrid nanofluid. In order to control the transport of industrial fluid it is very significant to use modified nanofluids because of large solid volume fraction of nanoparticles the boost in the velocity is controlled in axial direction. From Fig. 4, it is observed that for increasing values of curvature parameter k, the symmetry in the axial velocity $u(\eta)$ at $\eta = 0$ is attained. For smaller values of k the velocity is asymmetry at the heart of the channel due to pressure accelerated fluid layers near left boundary of the curved channel. The behavior is similar for all types of nanofluids but the effects disappear for modified hybrid nanofluid. Figs. (5-6) are presented to examine the response of flow patterns against the rising values of Hartman number for CuO / H_2O nanofluid and modified hybrid nanofluid. The rise in Hartman number results in the disappear of trapping bolus in the right half of the channel and formation of bolus occur in the left half of the channel for CuO / H_2O nanofluid and modified hybrid nanofluid. Furthermore, the size of bolus is large for modified hybrid nanofluid as compared to the CuO / H_2O modified hybrid nanofluid. This means that the more fluid is trapped in case of modified hybrid nanofluid in present study. The thermal Grashof number has also similar effect on the

trapping phenomena for both CuO/H_2O nanofluid and hybrid nanofluid as presented in Figs. (7-8). The streamlines for both curved channel $(k=3.0)$ and straight channel $(k=\infty)$ are presented in Figs. 9-10 for CuO/H_2O nanofluid $(\phi_1=0.04,\phi_2=0=\phi_3)$ and modified hybrid nanofluid $(\phi_1=0.04,\phi_2=0.05=\phi_3)$. The symmetry in the size of the bolus is observed for the straight channel i.e. $(k=\infty)$ as compared to curved channel $k=3.0$. The axial pressure against the rising values of Hartman number Ha, thermal Grashof number Gr_t and curvature parameter are presented in Figs. (11-13) for all types of nanofluids. It is noted that the rise in Hartman number the axial pressure rises and the rise in maximum for modified hybrid nanofluid. The similar trend is noted for axial pressure against the rising values of thermal Grashof number. Furthermore, the rising trend in axial pressure can be controlled for the curved channel instead of straight channel.

4.2 Heat transfer analysis

The temperature distribution $\theta(\eta)$ is plotted against the rising values of Hartman number Ha, thermal Grashof number Gr_t and curvature parameter k for CuO/H_2O nanofluid, hybrid nanofluid and modified hybrid nanofluid in Figs. (14-16). Hartman number cause a remarkable decline in the temperature of all types of nanofluids in a curved channel. The decline in temperature $\theta(\eta)$ is maximum for modified hybrid nanofluid as compared to the other types of nanofluids. The Lorentz force reduces the internal kinetic energy of nanofluid with large in case of modified hybrid nanofluid. Similar trend is noted for the temperature distribution of all types of nanofluids in curved configuration against boosting the thermal Grashof number which dominates the thermal buoyancy forces over the viscous forces and as a result the flow resistance is negligible. As a result, the internal kinetic energy falls and temperature profiles declines. Fig. 16 shows that the temperature is maximum in the curved channel as compared to straight channel. Furthermore, for CuO/H_2O nanofluid the temperature is maximum in the right half and for modified hybrid nanofluid the temperature is maximum in left half of the channel. The heat transfer coefficient against the rising values of Hartman number Ha, thermal Grashof number Gr_t and curvature parameter k for all types of nanofluids through Figs. (17-19). It is noted that the heat transfer rate is increasing function of Hartman number while decreasing function for thermal Grashof number and

curvature parameter. Also, it is noted that heat transfer rate is large for CuO / H_2O nanofluid while it is small for hybrid nanofluid and modified hybrid nanofluid.

5. Summarized findings

A computational investigation is worked out for complex channel flow of modified hybrid nanofluid due to peristaltic transport. The inspection of heating phenomenon is done in view of three nanoparticles like copper (CuO), copper oxide (CuO) and aluminium oxide (Al_2O_3) with water (H_2O) as a base fluid. A comparison for thermal results of nanofluid, hybrid model and modified hybrid nanofluid are developed. The numerical based treatment of model is suggested via shooting technique. Key results are:

- The axial velocity decreases in the left half of the channel and rises up to the right boundary by rising the Hartman number and thermal Grashof number.
- A symmetry is achieved at the heart of the channel for the rising values of curvature parameter.
- The number of trapping bolus increases in the left half of the channel by increasing Hartman number and thermal Grashof number.
- The symmetry in the size of trapping bolus is noted for straight channel.
- Axial pressure is minimum for curved channel and it rises for curved channel.
- The axial pressure is maximum for modified hybrid nanofluid as compared to other types of fluids.
- The heat transfer rate is minimum for modified hybrid nanofluid as compared to hybrid nanofluid.
- The heat transfer coefficent is more impressive for modifed hybrid nanofluid as compared to hybird nanoparticles.

References

1. Choi, S.U.S. “Enhancing thermal conductivity of fluids with nanoparticles” *ASME-Publications-Fed.* **231**, pp. 99-106 (1995).
2. Boungiorno, J., “Convective transport in nanofluids” *J. Heat. Transfer.* **128**, pp. 240-50 (2010)..
3. Turkyilmazoglu, M. “Single phase nanofluids in fluid mechanics and their hydrodynamic linear stability analysis” *Comput. Meth. Prog. Bio.* **187**, pp.105171 (2020).

4. Khan, S. U., Shehzad, A. "Brownian movement and thermophoretic aspects in third grade nanofluid over oscillatory moving sheet" *Phys. Scr.* **94(9),** pp. 095202 (2019).

5. Ibrahim, W., Gizewu, T. "Tangent hyperbolic nanofluid with mixed convection flow: an application of improved Fourier and Fick's diffusion model", *Heat Trans Asian Res.* **48**, pp. 4217-4239 (2019).

6. Tayebi, T., Chamkha, A.J., Djezzar, M. "Natural convection of CNT-water nanofluid in an annular space between confocal elliptic cylinders with constant heat flux on inner wall", *Sci. Iran. B,* **26(5),** pp. 2770-2783 (2019).

7. Hayat, T., Masood, F., Qayyum, S., et al. "Novel aspects of Soret and Dufour in entropy generation minimization for Williamson fluid flow", Scientia *Sci. Iran. B,* **27(5),** pp. 2451-2464 (2020).

8. Khan, S. U., Waqas, H., Muhammad, T., et al. "Simultaneous effect of bioconvection and velocity slip in three-dimensional flow of Eyring-Powell nanofluid with Arrhenius activation energy and binary chemical reaction" *Int. Commun. Heat Mass Transf.* **117**. pp.104738 (2020).

9. Khan, M. N., Nadeem, S., Ullah, N., et al. " Theoretical treatment of radiative Oldroyd-B nanofluid with microorganism pass an exponentially stretching sheet", *Surf. Interfaces,* **21**, pp. 100686 (2020).

10. Mondal. S., Pal., (2020). Computational analysis of bioconvective flow of nanofluid containing microorganisms over a nonlinear stretching sheet with variable viscosity using HAM. *J. compute. Des. Eng.* **7(2),** pp. 251-267.

11. Gowda, R.J. P., Kumar, R. N., Aldalbahi, A., et al. "Thermophoretic particle deposition in time-dependent flow of hybrid nanofluid over rotating and vertically upward/downward moving disk", *Surf. Interfaces*, **22**, pp. 100864 (2021).

12. Acharya, N. (2022), Impacts of different thermal modes of multiple obstacles on the hydrothermal analysis of Fe_3O_4–water nanofluid enclosed inside a nonuniformly heated cavity, *Heat Transfer,* **51(2)**, pp. 1376-1405.

13. Patil, P.M., Kulkarni, M., Tonannavar, J.R. "A computational study of the triple-diffusive nonlinear convective nanoliquid flow over a wedge under convective boundary constraints", *Int. Commun. Heat Mass Transf.* **128**, pp. 105561 (2021).

14. Patil, P.M., Shankar, H.F., Hiremath, P.S., et al. "Nonlinear mixed convective nanofluid flow about a rough sphere with the diffusion of liquid hydrogen"**,** *Alex. Eng. J.* **60(1),** pp. 1043-1053 (2021).

15. Acharya, N. “Buoyancy driven magnetohydrodynamic hybrid nanofluid flow within a circular enclosure fitted with fins”, *Int. Commun. Heat Mass Transf.* **133**, pp. 105980 (2022).
16. Madhukesh, J. K., Kumar, N. R., Gowda, R. J. P., et al. “Numerical simulation of AA7072-AA7075/water-based hybrid nanofluid flow over a curved stretching sheet with Newtonian heating: A non-Fourier heat flux model approach”, *J. Mol. Liq.* **335**, pp. 116103 (2021).
17. Sannad, M., Hussein, A. K., Abidi, A., et al. “Numerical Study of MHD Natural Convection inside a Cubical Cavity Loaded with Copper-Water Nanofluid by Using a Non-Homogeneous Dynamic Mathematical Model”, *Mathematics,* **10(12),** pp. 2072 (2022).
18. . Ali, , Mousa, A. A. A., Hammouch, Z., et al. “Insight into significance of thermal stratification and radiation on dynamics of micropolar water based TiO_2 nanoparticle via finite element simulation”, *J. Mater. Res. Technol.* **19**, pp. 4209-4219 (2022).
19. Hassan, M., El-Zahar, E.R., Khan, S. U., et al. “Boundary layer flow pattern of heat and mass for homogenous shear thinning hybrid-nanofluid: An experimental data base modeling”, *Numer. Methods Partial Differ. Equ.* **37(2),** pp. 1234-1249 (2021).
20. Bhatti, M. M., Abdelsalam, S. I., “Bio-inspired peristaltic propulsion of hybrid nanofluid flow with Tantalum (Ta) and Gold (Au) nanoparticles under magnetic effects” Waves Random Complex, https://doi.org/10.1080/17455030.2021.1998728 (2021).
21. Hamrelaine, S., Kezzar, M., Sari, M. R., et al. “Analytical investigation of hydromagnetic ferro-nanofluid flowing via rotating convergent/divergent channels”, *Eur. Phys. J. Plus.* **137**, pp. 1291 (2022).
22. Shahzad, F., Jamshed, W., Eid, M. R., I et al. “The effect of pressure gradient on MHD flow of a tri-hybrid Newtonian nanofluid in a circular channel”, *J. Magn. Magn. Mater*. **568**, pp. 170320 (2023).
23. Sajid, T., Jamshed, W., Ibrahim, R. W., et al. “Quadratic regression analysis for nonlinear heat source/sink and mathematical Fourier heat law influences on Reiner-Philippoff hybrid nanofluid flow applying Galerkin finite element method”, *J. Magn. Magn. Mater*. **568**, pp. 170383 (2023).
24. Hanif, H., Jamshed, W., Eid, M. R., et al. “Numerical Crank-Nicolson methodology analysis for hybridity aluminium alloy nanofluid flowing based-water via stretchable

horizontal plate with thermal resistive effect", *Case Stud. Therm. Eng.* **42**, pp. 102707 (2023).

25. Sajid, T., Pasha, A. A., Jamshed, W., et al. " Radiative and porosity effects of trihybrid Casson nanofluids with Bödewadt flow and inconstant heat source by Yamada-Ota and Xue models", *Alex. Eng. J.*. **66**, pp. 457-473 (2023).
26. Patil, P.M., Goudar, B. "Time-dependent mixed convection flow of Ag–MgO/water hybrid nanofluid over a moving vertical cone with rough surface", *J. Therm. Anal. Calorim.* **147**, pp. 10693–10705 (2022).
27. Patil, P.M., Shankar, H.F., Sheremet, M.A. "Mixed Convection of Silica–Molybdenum Disulphide/ Water Hybrid Nanoliquid over a Rough Sphere. *Symmetry*, **13**, pp. 236 (2021).
28. Patil, P.M., Shankar, H.F. (2022). Heat transfer attributes of Al_2O_3-Fe_3O_4/H_2O hybrid nanofluid flow over a yawed cylinder", *Propuls. Power Res.* **11(3)**, pp. 416-429.
29. Patil, P.M., Benawadi, S. "Shape effects on the mixed convective hybrid nanoliquid flow over a rough slender cylinder with convective condition", *Waves Random Complex*, https://doi.org/10.1080/17455030.2022.2143930, (2022).
30. Abbasi, A., Gul, M., Farooq, W., et al. "A comparative thermal investigation for modified hybrid nanofluid model (Al2O3-SiO2-TiO2)/(C2H6O2) due to curved radiated surface", *Case Stud. Therm. Eng.* **37**, pp. 102295 (2022).
31. Abbasi, A., Al-Khaled, K., Khan, M. I., et al. "Optimized thermal investigation for the modified hybrid nanofluid (Al_2O_3, CuO, Cu) with nonlinear thermal radiation and shape features", *Case Stud. Therm. Eng.* **28**, pp. 101425 (2021).
32. Javid, K., Bilal, M., Ali , N., et al. "Thermal investigation of peristaltic pumping of modified hybrid nanofluid $(Al_2O_3 - TiO_2 - Cu)/H_2O)$ through a complex wavy convergent channel with electro-magneto-hydrodynamic phenomenon", *Proc. Inst. Mech. Eng. E*:https://doi.org/10.1177/09544089221076592 (2022).
33. Ramesh, K., Tripathi, D., Bhatti, M. M., et al. "Electro-osmotic flow of hydromagnetic dusty viscoelastic fluids in a microchannel propagated by peristalsis", *J. Mol. Liq.* **314**, pp. 113568 (2020).
34. Rafaqat, R., Khan, A. A., Zaman, A., et al. "Magneto-hydrodynamics second grade compressible fluid flow in a wavy channel under peristalsis: Application to thermal energy", *J. Energy Storage*, **51**, pp. 104463 (2022).

35. Ullah, I., Shah, S. I., Alam, M. M., et al. " Thermodynamic of Ion-slip and magnetized peristalsis channel flow of PTT fluid by considering Lorentz force and Joule heating", *Int. Commun. Heat Mass Transf.* **136**, pp. 106163 (2022).
36. Bibi, A. Xu, H. "Entropy Generation Analysis of Peristaltic Flow and Heat Transfer of a Jeffery Nanofluid in a Horizontal Channel under Magnetic Environment", *Math. Probl. Eng.* **2019**, pp. 2405986 (2019).
37. Ali, A., Ali, Y., Marwat, D. et al. "Peristaltic flow of nanofluid in a deformable channel with double diffusion", *SN Applied Sci.* **2,** pp. 100 (2020).
38. Tripathi, D., Bég, O. A. "A study on peristaltic flow of nanofluids: Application in drug delivery systems", *Int. J. Heat Mass Transf.* **70**, pp. 61-70 (2014).
39. Tanveer, A., Malik, M.Y., "Slip and porosity effects on peristalsis of MHD Ree-Eyring nanofluid in curved geometry", *Ain Shams. Eng. J.* **12(1),** pp. 955-968 (2021).
40. Bibi, A., Xu, H. Peristaltic channel flow and heat transfer of Carreau magneto hybrid nanofluid in the presence of homogeneous/heterogeneous reactions. *Sci. Rep.* **10**, 11499 (2020).
41. Tanveer, A., Hayat, T., Alsaedi, A. "Numerical simulation for peristalsis of Sisko nanofluid in curved channel with double-diffusive convection", *Ain Shams. Eng. J.* **12(3)**, pp. 3195-3207 (2021).
42. Alhazmi, S. E., Imran, A., Awais, M., et al. "Thermal convection in nanofluids for peristaltic flow in a nonuniform channel", *Sci. Rep.* **12**, pp.12656 (2022).
43. McCash, L. B., Akhtar, S., Nadeem, S., et al. "Entropy Analysis of the Peristaltic Flow of Hybrid Nanofluid Inside an Elliptic Duct with Sinusoidally Advancing Boundaries", *Entropy (Basel).* **23(6)**, pp. 732 (2021).
44. Nadeem, S., Qadeer, S., Akhtar, S., et al. "Eigenfunction expansion method for peristaltic flow of hybrid nanofluid flow having single-walled carbon nanotube and multi-walled carbon nanotube in a wavy rectangular duct", *Sci. Prog.*. **104(4)**, pp. 1-14 (2021).
45. McCash, L. B., Akhtar, S., Nadeem, S., et al. "Entropy Analysis of the Peristaltic Flow of Hybrid Nanofluid Inside an Elliptic Duct with Sinusoidally Advancing Boundaries", *Entropy*, **23**, pp. 732 (2021).

Nomenclature

$\bar{t}$ time (s^{-1})

μ_m viscosity ($kgm^{-1}s^{-1}$)

ρ_m density (kg/m^3)

$(\bar{R}, \bar{X})$ orthogonal curvilinear coordinates (m)

$\bar{T}$ temperature (K)

$\bar{U}, \bar{V}$ components of velocity (ms^{-1})

μ_m dynamic viscosity $(kgm^{-1}s^{-1})$

$\bar{P}$ pressure (m^2)

K_m thermal conductivity (W/mK)

σ_m electric conductivity (S/m)

c speed of sinusoidal wave

λ wave length

ζ phase difference

(σ, ω) geometrical parameters

R^* radius of curvature

$(\rho cp)_m$ heat capacity

$(\beta)_m$ thermal expansion coefficient of modified hybrid nanofluid.

m non-uniform parameter

E_C Eckert number

p_r Prandtl number

Gr_t thermal Grashof number

Ha Hartman number.

Table 1 Thermo-physical properties of base fluid and nanoparticles [21, 22].

Base fluid/Solid	H_2O	$CuO(\phi_1)$	$Cu(\phi_2)$	$Al_2O_3(\phi_3)$

particles				
ρ	997.1	6500	8933	3970
(C_p)	4180	540	385	765
K	0.6071	18	400	40
σ	5.5×10^{-6}	6.9×10^{-2}	59.6×10^{6}	35×10^{6}
β	210×10^{-6}	385×10^{-6}	531.8×10^{-6}	8.9×10^{-6}

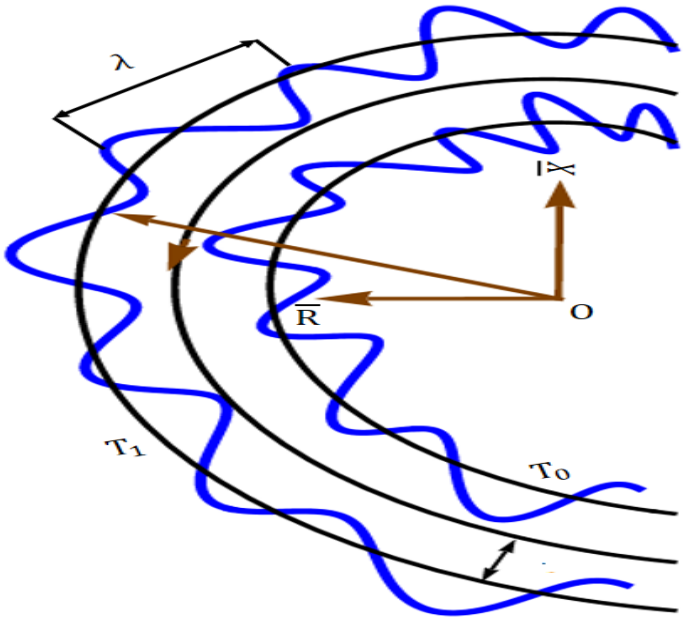

Fig. 1: Geometry of the Problem

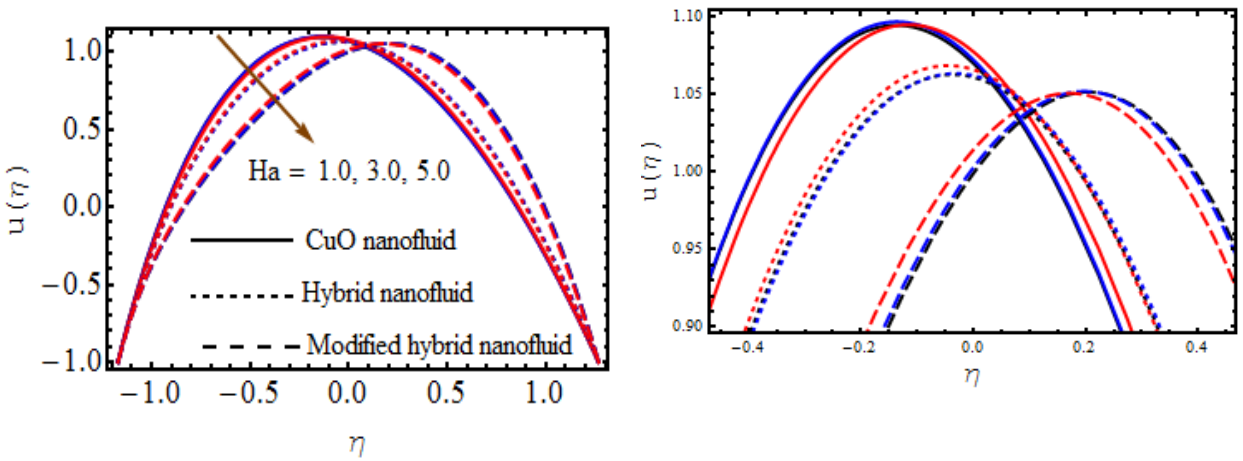

Fig. 2: Variation of axial velocity $u(\eta)$ against Ha with $m = 0.1, a_1 = 0.1, b_1 = 0.2, \sigma = 1 = \omega, x = 0.5, q = 1.0 = Gr_t = Br, k = 2.5$ and $\phi = \pi$.

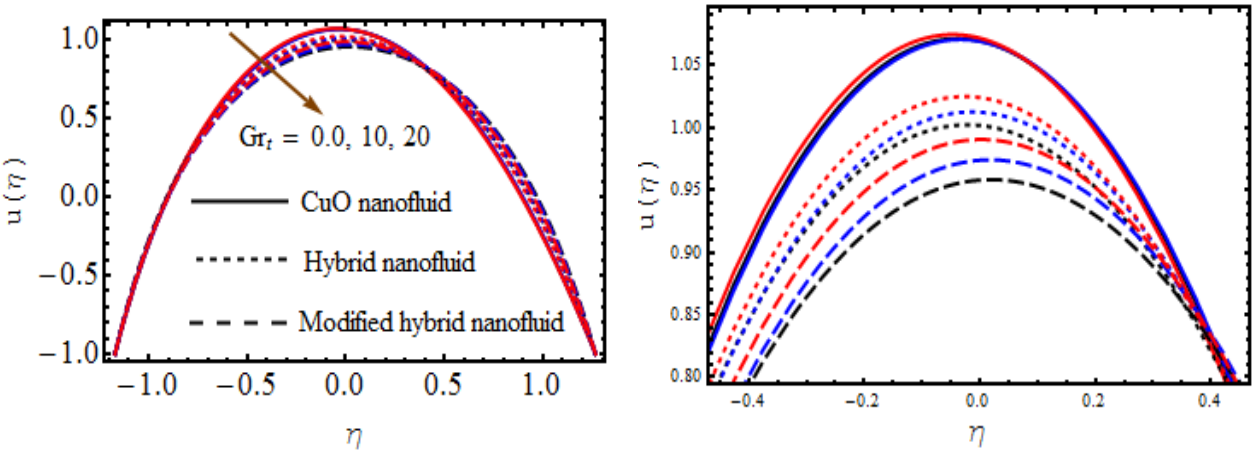

Fig. 3: Variation of axial velocity $u(\eta)$ against Gr_t with $m = 0.1, a_1 = 0.1, b_1 = 0.2, \sigma = 1 = \omega, x = 0.5, q = 1.0 = Br, Ha = 3.0, k = 2.5$ and $\phi = \pi$.

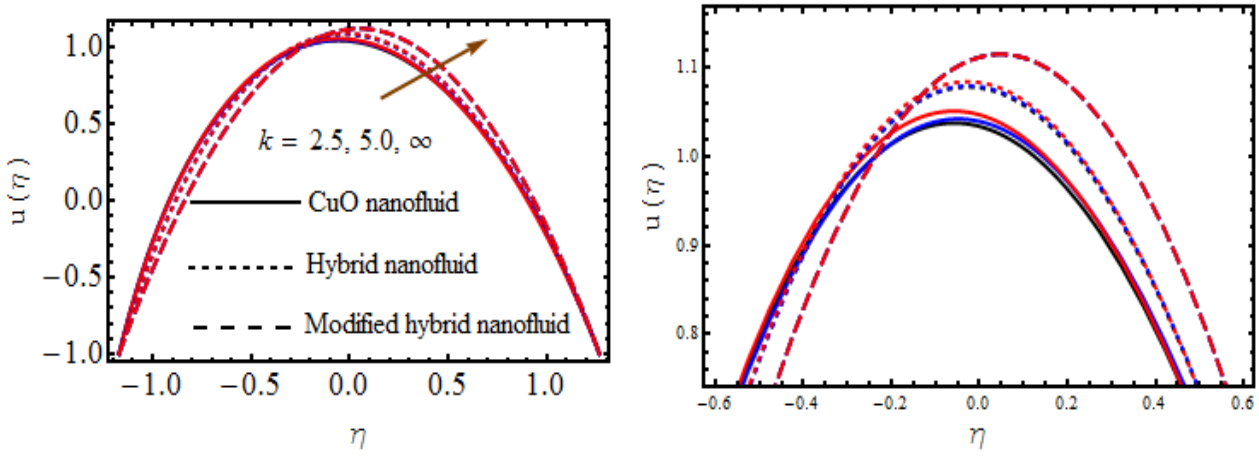

Fig. 4: Variation of axial velocity $u(\eta)$ against k with $m = 0.1, a_1 = 0.1, b_1 = 0.2, \sigma = 1.0 = \omega, x = 0.5, q = 1.0 = Br, Ha = 3.0, Gr_t = 2.0$ and $\phi = \pi$

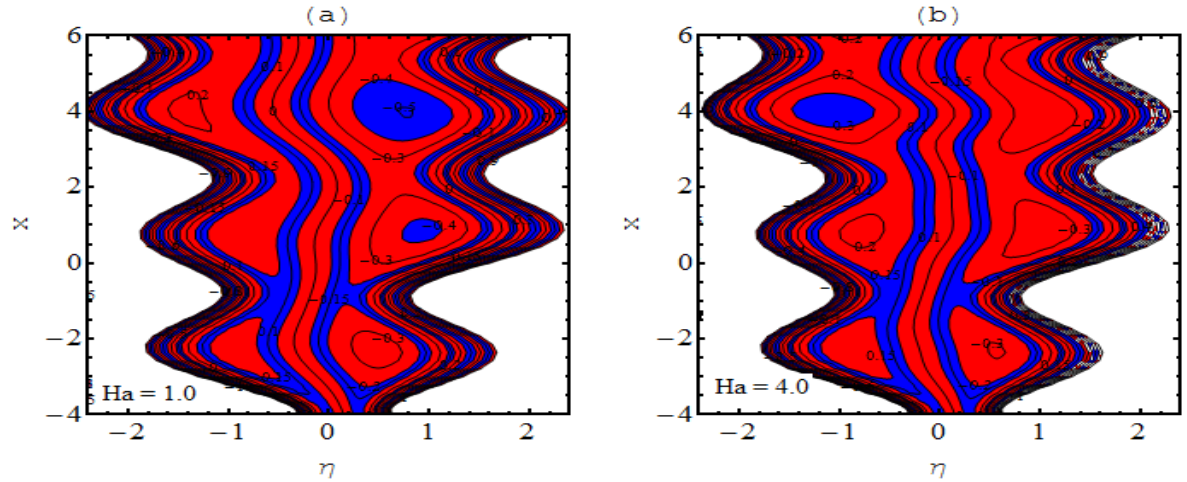

Fig. 5: Stream lines for $Ha = 1.0$ and $Ha = 4.0$ in CuO/H_2O nanofluid with $m = 0.1, a_1 = 0.2, b_1 = 0.4, \sigma = 1.0 = \omega, k = 3.0, q = 0.2, Gr_t = 1.0, Br = 0.5$ and $\phi = \pi$.

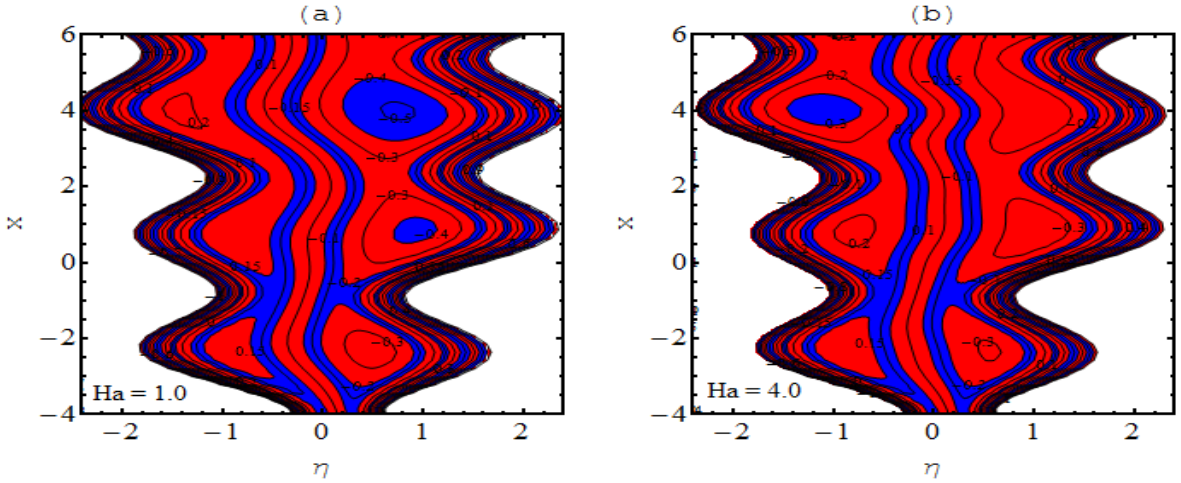

Fig. 6: Stream lines for $Ha = 1.0$ and $Ha = 4.0$ in modified hybrid nanofluid with $m = 0.1, a_1 = 0.2, b_1 = 0.4, \sigma = 1.0 = \omega, k = 3.0, q = 0.2, Gr_t = 1.0, Br = 0.5$ and $\phi = \pi$.

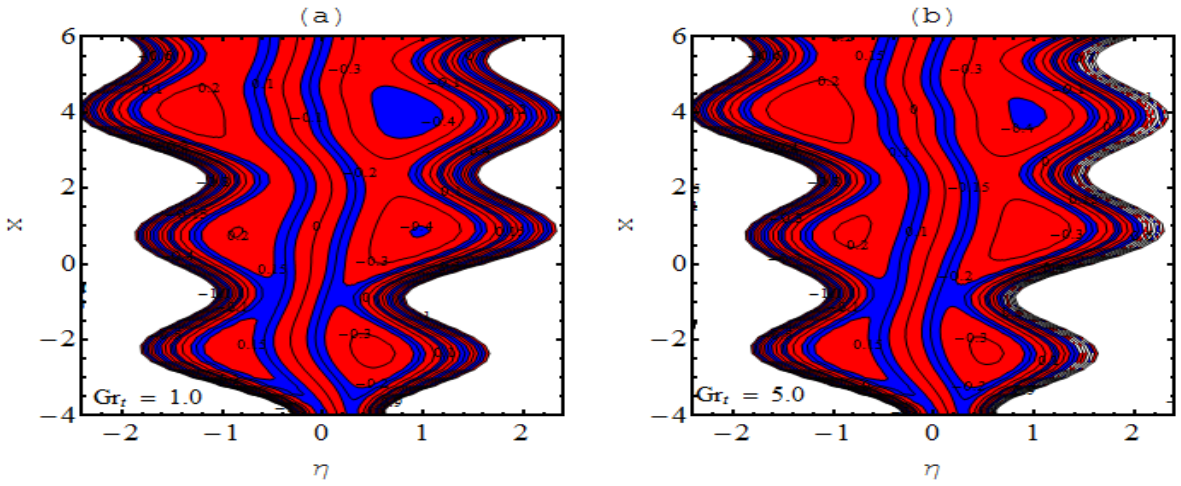

Fig. 7: Stream lines for $Gr_t = 1.0$ and $Gr_t = 5.0$ in CuO/H_2O nanofluid with $m = 0.1, a_1 = 0.2, b_1 = 0.4, \sigma = 1.0 = \omega, q = 0.2, Ha = 2.0, k = 3.0$ $Br = 0.5$ and $\phi = \pi$.

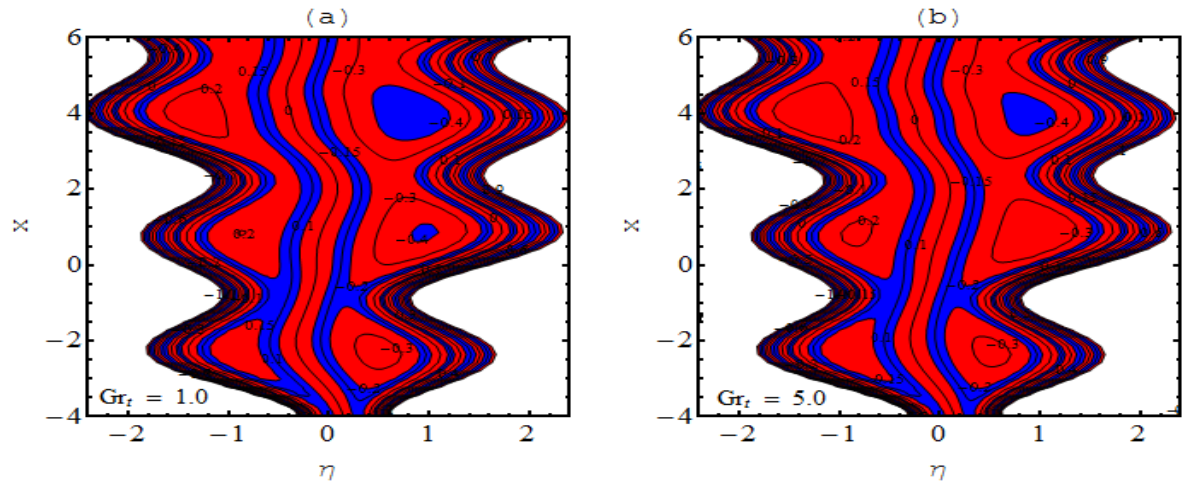

Fig. 8: Stream lines for $Gr_t = 1.0$ and $Gr_t = 5.0$ in modified hybrid nanofluid with $m = 0.1, a_1 = 0.2, b_1 = 0.4, \sigma = 1.0 = \omega, q = 0.2, Ha = 2.0, k = 3.0, Br = 0.5$ and $\phi = \pi$.

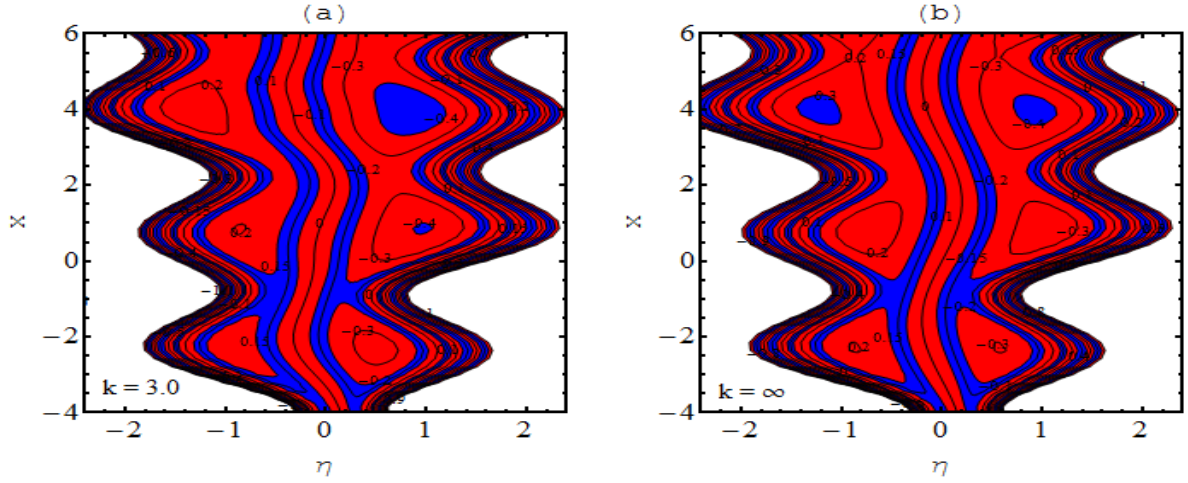

Fig. 9: Stream lines for $k = 3.0$ and $k = \infty$in CuO/H_2O nanofluid with $m = 0.1, a_1 = 0.2, b_1 = 0.4, \sigma = 1.0 = \omega, q = 0.2, Ha = 2.0, Br = 0.5, Gr_t = 1.0$ and $\phi = \pi$.

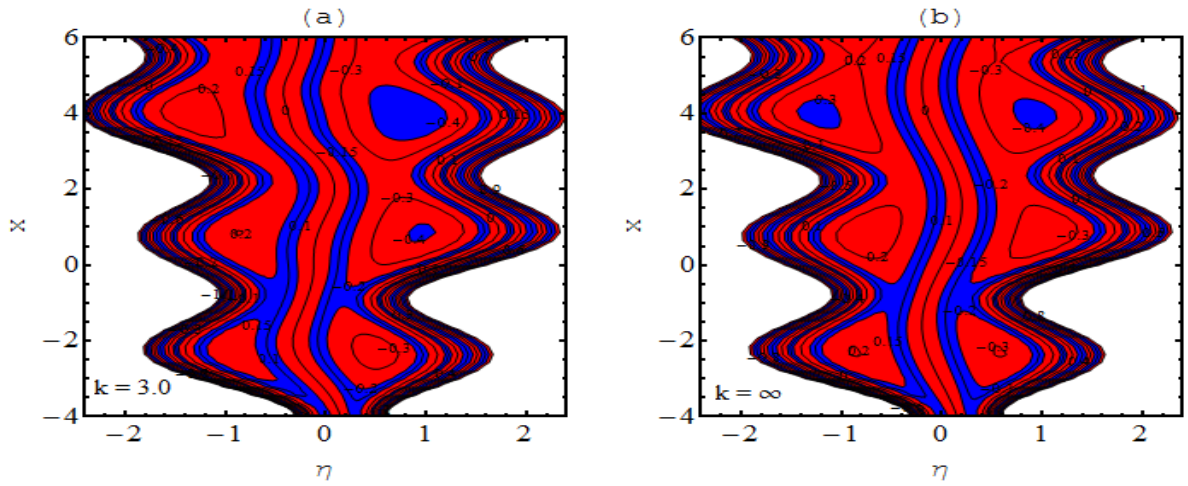

Fig. 10: Stream lines for $k = 3.0$ and $k = \infty$ in modified hybrid nanofluid with $m = 0.1, a_1 = 0.2, b_1 = 0.4, \sigma = 1.0 = \omega, q = 0.2, Ha = 2.0, Br = 0.5, Gr_t = 1.0$ and $\phi = \pi$.

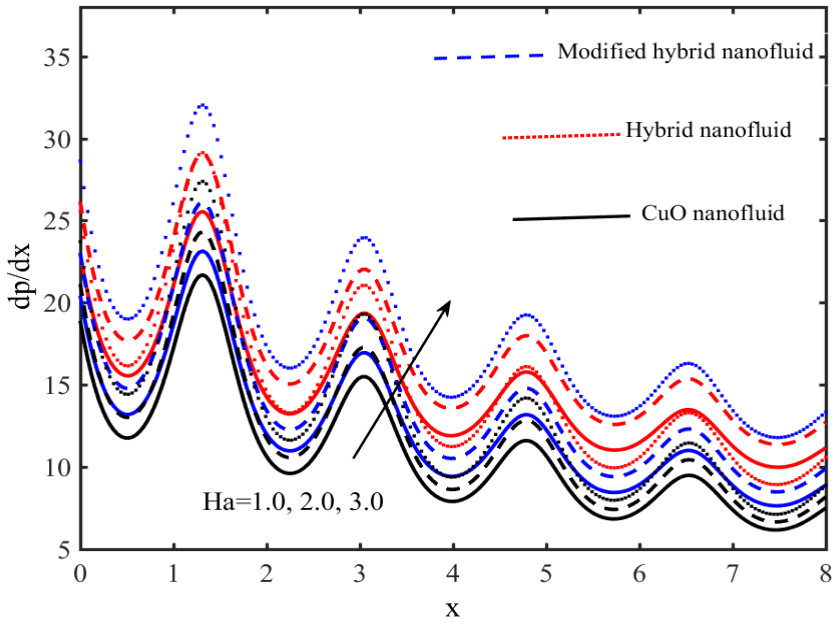

Fig. 11: Variation of axial pressure dp/dx against Ha with $m = 0.1, a_1 = 0.1, b_1 = 0.2, \sigma = 1.0 = \omega, q = 0.2, k = 3.0, Br = 1.0, Gr_t = 1.0$ and $\phi = \pi$.

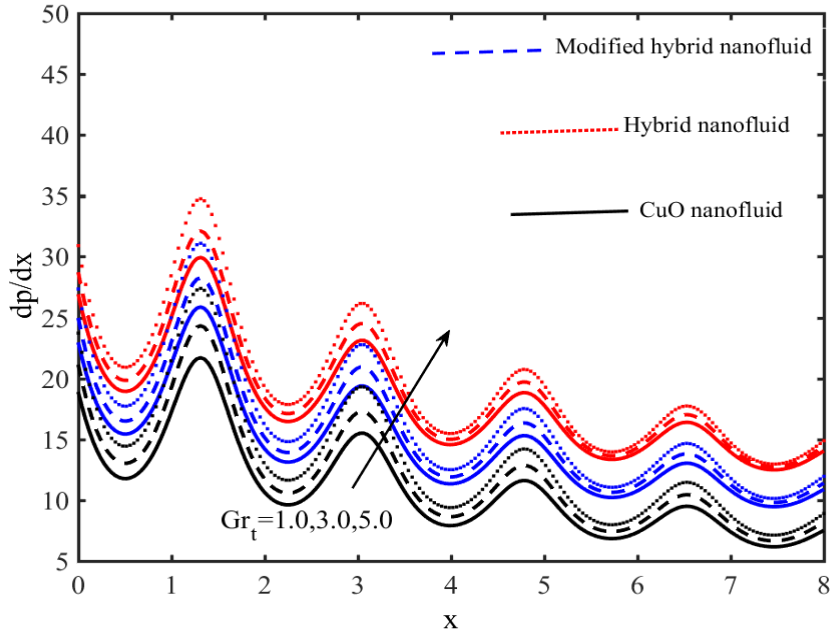

Fig. 12: Variation of axial pressure dp/dx against Gr_t with $m = 0.1, a_1 = 0.1, b_1 = 0.2, \sigma = 1.0 = \omega, q = 0.2, k = 3.0, Br = 1.0, Ha = 1.0$ and $\phi = \pi$.

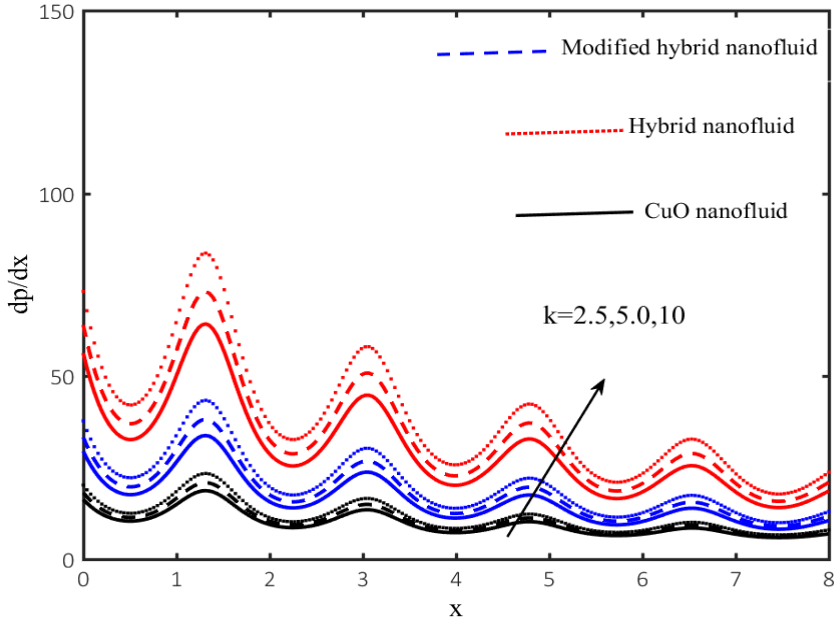

Fig. 13: Variation of axial pressure dp/dx against k with $m = 0.1, a_1 = 0.1, b_1 = 0.2, \sigma = 1.0 = \omega, q = 0.2, Ha = 1.0, Br = 1.0, Ha = 1.0$ and $\phi = \pi$.

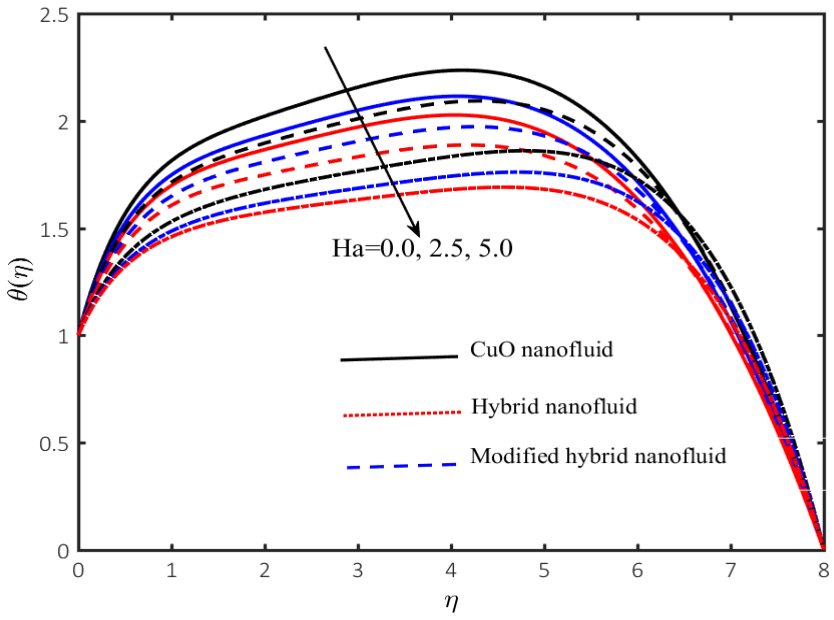

Fig. 14: Variation of temperature $\theta(\eta)$ against Ha with $m = 0.1, a_1 = 0.1, b_1 = 0.2, \sigma = 1.0 = \omega, x = 0.5, q = 1.0 = Gr_t = Br, k = 2.5$ and $\phi = \pi$.

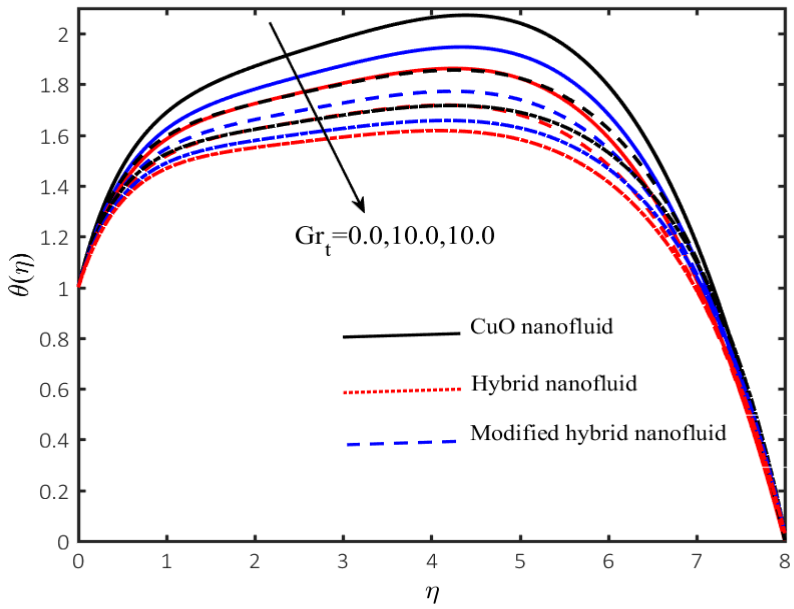

Fig. 15: Variation of temperature $\theta(\eta)$ against Gr_t with $m = 0.1, a_1 = 0.1, b_1 = 0.2, \sigma = 1.0 = \omega, x = 0.5, q = 1.0 = Br, Ha = 3.0, k = 2.5$ and $\phi = \pi$.

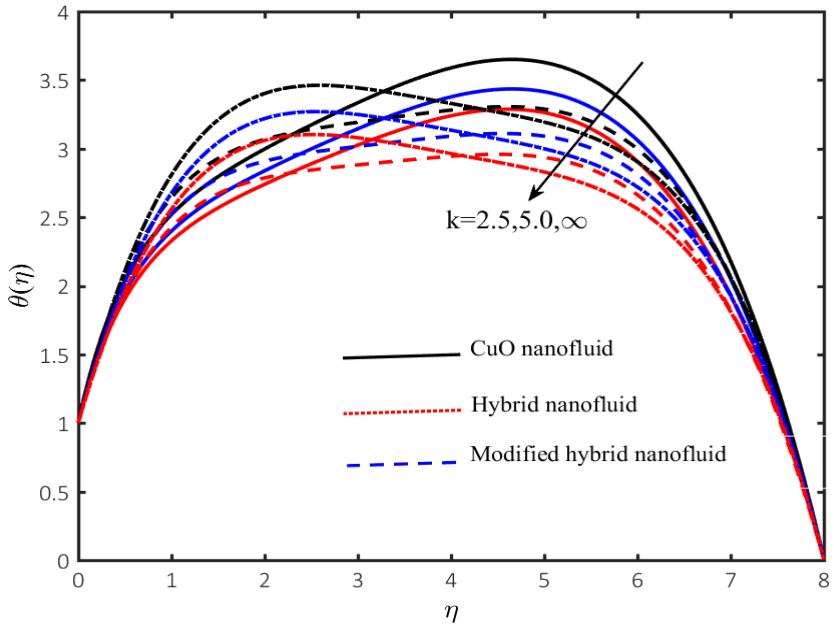

Fig. 16: Variation of temperature $\theta(\eta)$ against k with $m = 0.1, a_1 = 0.1, b_1 = 0.2, \sigma = 1.0 = \omega, x = 0.5, q = 1.0 = Br, Ha = 3.0, Gr_t = 2.0$ and $\phi = \pi$.

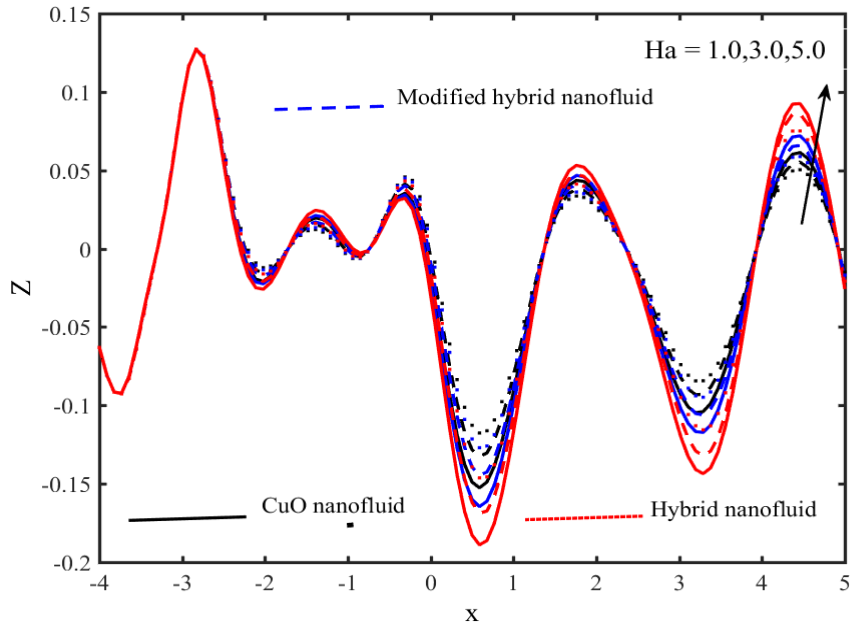

Fig. 17: Variation of heat transfer coefficent Z against Ha with $m = 0.1, a_1 = 0.1, b_1 = 0.2, \sigma = 1.0 = \omega, q = 1.0 = Gr_t = Br, k = 2.5$ and $\phi = \pi$.

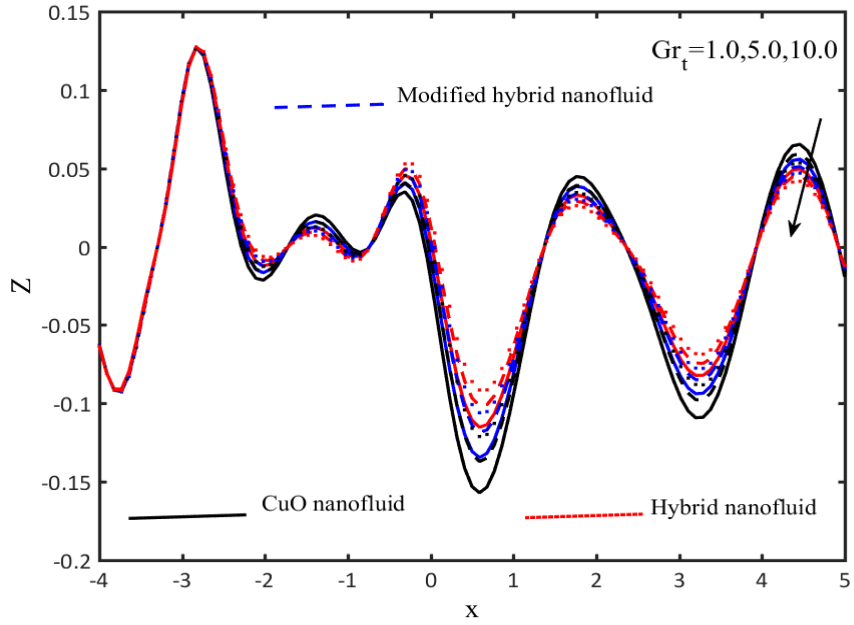

Fig. 18: Variation of heat transfer coefficent Z against Gr_t with $m = 0.1, a_1 = 0.1, b_1 = 0.2, \sigma = 1.0 = \omega, q = 1.0 = Br, k = 3.0, Ha = 2.0$ and $\phi = \pi$.

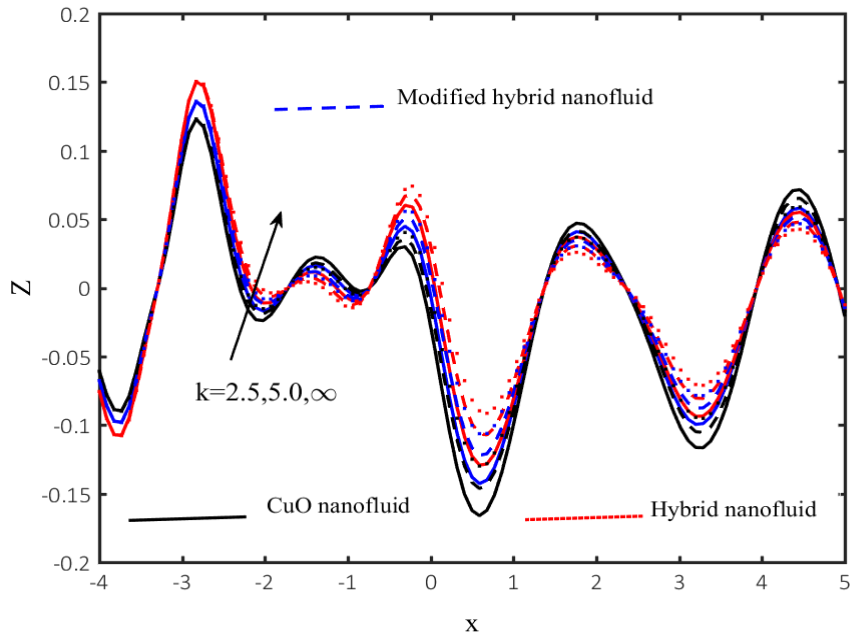

Fig. 19: Variation of heat transfer coefficent Z against k with $m = 0.1, a_1 = 0.1, b_1 = 0.2, \sigma = 1.0 = \omega, q = 1.0 = Br, Ha = 2.0, Gr_t = 10$ and $\phi = \pi$.

Biographies

Imtiaz Ahmed is working in Mirpur university of Science and Technology, Mirpur Pakistan. Dr. Ahmed has published 53 research paper with impact factor 80 plus. His area of research is fluid mechanics and nanofluids. He is reviewer of 20 impact factor journals.

Shahid Hameed is assistant professor in Mirpur university of Science and Technology, Mirpur Pakistan. Shahid Hameed area of interest is nanofluids and partial differential equations. He has published 20 research papers with impact factor 35.43. He is reviewer of 25 international journals.

Aamar Abbasi is assistant professor in the University of Azad Jammu and Kashmir Muzaffarabad, Pakistan. Dr Abbasi is working in nanofluids and heat and mass transfer problems. He is published 75 research papers in well reputed international journals.

Sami Ullah Khan is Associate Professor in the Namal University Mianwali Pakistan. Dr. Khan has published 370 research papers with impact factor 1000 plus. He is reviewer of more than 70 impact factor journal. Dr Khan is guest editor of 4 impact factor journals. Dr Khan has been awarded as distinguish researcher from university.

Waseh Farooq is PhD student in the University of Azad Jammu and Kashmir Muzaffarabad, Pakistan. Waseh Farooq is working in thermal engineering. Waseh Farooq has published 31 research papers. His research interest area includes numerical analysis and nanofluids.

Mohammed A. Almeshaal is Professor in Imam Mohammad Ibn Saud Islamic University, Riyadh Saudi Arabia. His area of interest is nanotechnology. Dr. Almeshaal has more than 15 years of teaching an research experiences. Dr. Almeshaal has published 20 research articles in different journals.

Muapper Alhadri is associate professor University of Ha'il, Ha'il City, Saudi Arabia. Dr. Alhadri has received PhD degree in mechanical engineering. His research expertise is in fluid mechanics and numerical analysis. Dr. Alhadri has published 36 research papers. He is also reviewer of many international journals.

Lioua Kolsi is an associate Professor in the University of Hail, Saudia Arabia. Dr Kolsi is working in thermal systems and published more than 300 research papers in different journals. His area of research is nanofluids, thermal engineering and computational fluid mechanics. Dr Kolsi is guest editor of applied sciences journal.